Footprint Catalysis. XI.[1—10] Molecular Footprint Cavities Imprinted with Chiral Amines and Their Chiral Molecular Recognition

Kensaku MORIHARA,* Michie TAKIGUCHI, and Toyoshi SHIMADA
Department of Chemistry, Faculty of Science, Nara Women's University, Kitauoyanishi-machi, Nara 630
(Received August 11, 1993)

Chiral amines, (*R*)- and (*S*)-*N*-benzyl-α-methylbenzylamine, served as templates in a molecular imprinting we developed. They formed "molecular footprint" cavities on a silica (alumina) gel surface, which showed catalytic activities toward transacylation of benzoic anhydride. The catalyses were susceptible to enantioselective inhibitions by the rebinding of the chiral template amines. This finding proved that the cavities could show chiral recognition through their chirally marked cavity structures.

There are many chiral amines in natural products and synthetic medicines that have significant physiological actions. In some cases, their stereoisomers show varying physiological effects. Therefore, precise analysis and effective isolation of them would be a very important issue for medicinal chemistry. Recently K. Mosbach et al. reported a chromatographic resolution of racemic β-adrenergic blockers using chirally imprinted polymers prepared by molecular imprinting.[13]

We developed our original molecular imprinting procedures; an imprinting with a template can form "molecular footprint"-like cavities on a silica (alumina) gel surface.[1—12] During our studies on catalytic behavior of the footprint cavities, we found chirally imprinted cavities showed enantioselective catalyses based on their chiral recognition.[6,9,11,12] We applied these chiral recognition capabilities to analysis and separation of chiral amines. In this paper, we report on the chiral recognition of molecular footprints imprinted with (*R*)- and (*S*)-*N*-benzyl-α-methylbenzylamine. The silica (alumina) gel samples imprinted with a template were characterized by the usual method, i.e., analysis of their catalytic behavior on 2,4-dinitrophenolysis of benzoic anhydride. The rebinding of the chiral amines used as templates enantioselectively inhibited the catalyses. This finding meant that "free" amine bases formed molecular footprint cavities for the first time, and that they had chiral complementary structures as expected.

Experimental

Apparatus: Shimadzu UV-160 gave absorption spectra. Horiba F-7 with #6326 electrode measured pHs.

Materials: All chemicals were of guaranteed grade from Nacalai Tesque Co. Ltd., if not specified.

Silica Gel: Merck Kieselgel 60, art. No. 7754, particle size 0.06—0.20 mm, mesh 70—230, was used.

Templates: (*R*)-(+)-*N*-Benzyl-α-methylbenzylamine **1** and (*S*)-(−)-*N*-benzyl-α-methylbenzylamine **2** were products of JPS Chimie. (*R*)-(+)-α-Methylbenzylamine **3** and (*S*)-(−)-α-methylbenzylamine **4** were products (98%) of Aldrich. All of them were used without further purification.

Substrate: Benzoic anhydride was recrystallized from benzene–petr. benzin, mp 42 °C.

Solvent: Acetonitrile, dehydrated over calcium chloride in advance, was dried over phosphorus pentaoxide overnight. It was distilled using a Hempel fractionating column, bp 81—82 °C. To the distillate was added calcium hydride, and repeated distillation gave water- and acidic impurity-free acetonitrile.[3]

Nucleophile: Potassium 2,4-dinitrophenolate, prepared by neutralization of 2,4-dinitrophenol in methanol with conc aqueous potassium hydroxide, was recrystallized from hot water, and dried at 130 °C in vacuo.[3]

Catalyst Preparation: The preparation procedures were the same as those previously reported in detail.[3,7] They included successive surface activation, aluminium ion doping, imprinting with templates, drying, and methanol extraction. Kieselgel (100 g) was refluxed with conc hydrochloric acid (400 cm^3) for 4 h to activate the gel surface for silanol groups. The gel was repeatedly washed with deionized water until the washing reach nearly pH 6.0. Then it was washed with dil aqueous ammonia of pH 7—8 three times, and again washed with water three times. This will be referred to as "blank gel" later in the text. To the washed gel sludge was added an aqueous solution of aluminium chloride (0.2 mol dm^{-3}, 50 cm^3 to 10 g dry weight of the gel). The pH of the mixture was adjusted to pH 6.5 with dil aqueous ammonia. The mixture was kept at 80 °C for 3 h. This Al^{3+} ions doping should cause an isomorphical substitution of silicate on the gel surface by aluminate to generate Lewis acid sites. The doped gel was isolated by decantation from precipitated aluminium hydroxide, and washed with dil hydrochloric acid (pH 4.0) until the supernatant became clear. Then it was imprinted with a template. To a gel portion (equivalent to 10 g of dry weight) was added an acetone solution of a template (1.5×10^{-3} mol in 10 cm^3 of acetone). The pH of the mixture was adjusted to pH 4.0 with dil hydrochloric acid. The mixture was kept at room temperature for a week with occasional pH adjustment. The gel sludge was isolated from the supernatant and the excess of the template deposited by decantation, and then washed with dil hydrochloric acid (pH 4.0) 10 times. The gel sludge was collected by filtration so carefully that the gel surface always was kept wet. Then it was dried on Petri dishes at room temperature until it reached a constant weight. It took about 7 days. The dried gel thus obtained was extracted with methanol using a Soxhlet extractor. It usually took 4—5 h. This continual

extraction caused forced removal of template molecules from the silicate surface, which left molecular footprint cavities on the surface. Finally the extracted gel preparation was dried, first in a desiccator at room temperature under atmospheric pressure overnight. Then it was exhaustively dried at 140 °C under reduced pressure (3 mmHg, 1 mmHg=133.322 Pa) for 1 h. The fully dried gel samples were immediately used for subsequent kinetic studies. Similar procedures, only omitting a template acetone, gave the control gel catalysts, which had only Lewis acid sites lacking complementary structures around them.

Kinetic Measurement: The catalytic activities of the gel were measured by 2,4-dinitrophenolysis of benzoic anhydride. The procedures were the same as those previously reported.[3] Acetonitrile solution of the substrate (49 cm^3, 0.9—4.5×10^{-3} mol dm^{-3}) was equilibrated with a catalyst (50 mg) at 30 °C for 30 min. To the mixture, was added the nucleophile solution (1 cm^3, 1.5×10^{-2} mol dm^{-3}) to start the reactions. The catalyzed reactions were followed by triple-wavelength spectrophotometry. The decreases in the optical density of the reaction mixtures at 400, 430, and 500 nm due to 2,4-dinitrophenolate were measured at proper intervals. Pseudo-first-order rate constants, k_{obsd} were calculated from the linear part of semi-log plots of optical density vs time that were usually observed over at least 1 half-life. The k_{obsd}s thus obtained obeyed Michaelis–Menten kinetics with respect to the substrate concentration. Kinetic parameters, K_ms (Michaelis constants) and V_{max}s (maximum k_{obsd}s) were calculated from the usual double reciprocal plots (Lineweaver–Burk plots). The catalytic rate constants, k_{cat}s, were calculated from V_{max} divided by catalytic sites molarity per gram.

In inhibition studies, the amine inhibitors caused an unexpected increase in the optical density at final stage of the catalyzed reaction (See text). A modification of the procedures for kinetic measurements was required as follows. Besides a sample of the imprinted catalyst (50 mg), a portion (50 mg) of a dried "blank gel" (See Experimental), was equilibrated with an acetonitrile solution of an inhibitor for 20—30 min. Then they were equilibrated with the substrate solutions for 10 min more. The subsequent procedures were the same as before. The inhibition constant K_i for a noncompetitive inhibition of the control catalyst was calculated from equation,[14] $\nu=k_{cat}[cat][S]/\{(1+[I]K_i^{-1})+(1+[I]K_i^{-1})K_m\}$. The inhibition constant K_i for a competitive inhibition by **2** or **3** was obtained from the equation,[14] $\nu=k_{cat}[cat][S]/K_m\{(1+[I]K_i^{-1})+[S]\}$. Also K_i for an "uncompetitive" inhibition by **3** or **4** was obtained from the equation,[14] $\nu=k_{cat}[cat][S]/\{(1+[I]K_i^{-1})[S]+K_m\}$, where [cat] was the molarity of the catalytic site; $k_{cat}[cat]$ was equal to $k_{obsd.max}$; [S] was the substrate concentration; [I] was the inhibitor concentration; k_{cat} and K_m were the same as those of the catalyzed reaction without the inhibitor.

Catalytic Sites Titration: Catalytic sites molarities were measured by the kinetic titration method previously reported.[3] This was based on irreversible poisoning of the catalytic sites with pyridine. The gel catalyst (50 mg) was equilibrated with specified amounts of pyridine in acetonitrile (5—15 cm^3, 5.0×10^{-5} mol dm^{-3}) at 30 °C for 1 h with gentle stirring. At this time irreversible poisoning proceeded completely to consume all free pyridine in the mixture. Then the catalytic activities by surviving catalytic sites were measured as usual, the total volume of reaction mixtures being kept to 50 cm^3. The k_{obsd}s obtained were plotted against pyridine molarity. Extrapolation of a linear plot gave an intercept on the abscissa. The numerical value of the intercept directly showed the molarity of the catalytic sites per 1 gram of catalyst, since pyridine in 50 cm^3 of the reaction mixtures poisoned a catalyst of 50 mg in these conditions.

Results and Discussion

Design of Catalysis System. We have studied the molecular recognition capabilities of several footprint cavities thus far according to a kinetic method.[2,4,5] The method depends on the competitive inhibition of the footprint-catalyzing reactions by the binding of the template used during imprinting and its related compounds. The free energy change $-\Delta G_0$ ($=RT$ ln K_i), calculated from the observed competitive inhibition constants K_is, measures the magnitude of the molecular recognition. The kinetic method measures the intrinsic molecular recognition capabilities of the footprint cavities. The other method based on an adsorption isotherm is less reliable because the nonspecific adsorption on the outer area would cover the intrinsic binding onto the footprint cavities. Therefore, this investigation used the kinetic method to measure the molecular recognition capability.

The kinetic method required a catalysis system to gain competitive inhibition constants, K_i. The design of the catalysis system might depend on how to choose proper template and how to assay the catalytic activities of the footprint cavities. The footprint imprinting was of the "tailor-made". Any compound of a Lewis base could serve as a template, if it was moderately insoluble in the imprinting conditions. For this fundamental study for chiral amines recognition we chose chiral amines, **1** and **2**, as templates. The reasons why we chose them were as follows. The amines, **1** and **2**, were commercial products for optical resolution, and both of the enantiomers were easily available with high optical purities (Scheme 1). They were amines of a free base, and this was the first use of a free base for the imprinting. Most of the templates used for imprinting thus far were acylamines, or diacylamines. So it would extend the scope of the template choice. The templates **1** and **2** involved two phenyl groups within the molecules, and had similar molecular size to benzoic anhydride. The similarities between the template molecules and benzoic anhydride in size and shape would give a good matching for the cavities with the substrate in the catalytic process. Thus the established 2,4-dinitrophenolysis of benzoic anhydride for the catalytic activity assay[3] could be available. Additionally, chiral amines of sufficient optical purities, **3** and **4**, that had the partial structures of **1** and **2**, were also easily available commercially. They could provide a tool for investigation of partial recognition capabilities.[3—5,10]

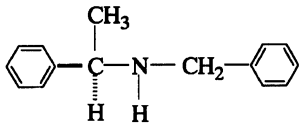

1

(*R*)-(+)-*N*-Benzyl-α-methylbenzylamine

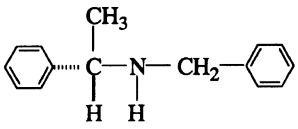

2

(*S*)-(-)-*N*-Benzyl-α-methylbenzylamine

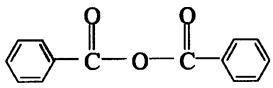

Benzoic anhydride : Substrate

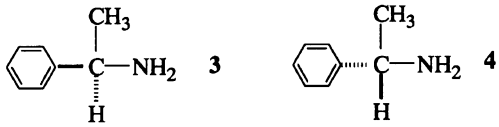

(*R*)-(+)-α-Methylbenzylamine 3 (*S*)-(-)-α-Methylbenzylamine 4

Scheme 1. Templates, substrate, and inhibitors.

Binding Capacities of the Imprinted Gel Preparations. Figure 1 shows the titration plots for the catalytic sites of the control catalyst, the imprinted catalysis with **1** (referred to as {*R*} from now on) and **2** ({*S*}). The titers were 2.22×10^{-5} mol g^{-1}, 2.30×10^{-5} mol g^{-1}, and 2.67×10^{-5} mol g^{-1}, respectively. The

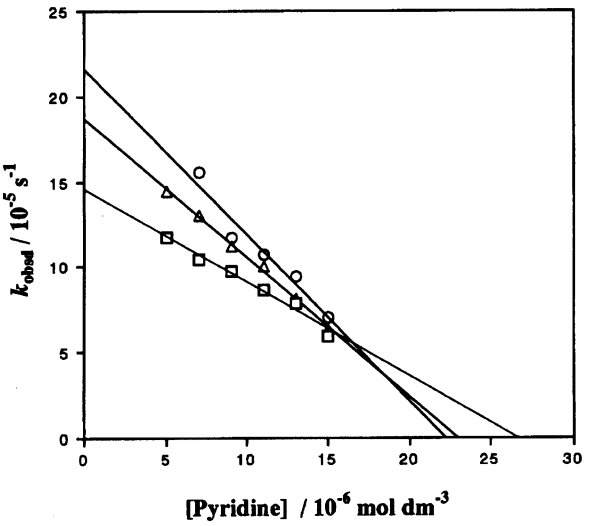

Fig. 1. Catalytic site titrations of the control catalyst and the imprinted catalysts, {*R*} and {*S*}. Substrate concentration: 1.8×10^{-3} mol dm^{-3}. Catalyst: 50 mg in 50 cm^3 of pyridine–acetonitrile solution. Open circle: The control catalyst, titer; 2.22×10^{-5} mol g^{-1}. Open triangle: The imprinted catalyst {*R*}, titer; 2.30×10^{-5} mol g^{-1}. Open square: The imprinted catalyst {*S*}, titer; 2.67×10^{-5} mol g^{-1}.

titers of the imprinted catalysts meant the binding capacities of the footprint cavities on the gel surface, and they were 4.85 mg of **1**/g, and 5.63 mg of **2**/g. The observed capacities were significantly higher than a high capacity (1.5 mg of *N*-phenyl-L-phenylalaninamide/g) of a methacrylic acid polymer prepared by molecular imprinting.[15]

Constant titers were reproducibly obtainable at the separate methanol extraction. The amine templates were more basic than acylamines and diacylamines usually used as templates, but the methanol extraction for 4—5 h seemed sufficient to remove the template perfectly.

Improved Procedures for Inhibition with the Amine Inhibitors. The inhibition reaction with an amine inhibitor showed anomalous behavior that decrease in the optical density and then increase again at the final stage (30—50 min) of the catalyzed reaction. Preliminary TLC experiments for product analysis suggested that the regeneration of 2,4-dinitrophenolate from the reaction product, 2,4-dinitrophenyl benzoate caused this increase in the optical density. The accumulated reaction product can react with the amine as the inhibitor to regenerate the 2,4-dinitrophenolate anion, since the amines themselves can act as nucleophiles. A device in the procedures can reduce the interference by the regeneration of 2,4-dinitrophenolate. The addition of the blank gel into the catalyzed reaction system was effective (See Experimental). The blank gel had no effect on the catalysis. It can nonspecifically adsorb the reaction product on the surface to prevent nucleophilic attack of the amine inhibitor. Thus it can remove the interference with the amine inhibitor from the inhibition studies.

Enantioselective Competitive Inhibition. Figure 2 shows the Lineweaver–Burk plots for the catalyzed reactions of the control gel catalyst. The plots evidently had a noncompetitive inhibition pattern in that three plotting lines made nearly identical intercepts on the abscissa within experimental error. The occurrence of noncompetitive inhibition meant that both (*R*)-template and (*S*)-template caused irreversible poisoning of the native Lewis acid sites on the surface of the control catalyst, such as pyridine poisoning. Since the Lewis acid sites of the control catalyst involved no chiral factor, no difference in the inhibitory effects of (*R*)-template and (*S*)-template was observed. Two plotting lines shown in Fig. 2 were identical within experimental error. Figures 3 and 4 show the Lineweaver–Burk plots for the reaction over the cavities {*R*} and {*S*}. These plots showed typical competitive inhibition patterns, in contrast to those in Fig. 2; three plotting lines made nearly identical intercepts on the vertical axis. The competition observed between the template molecules and the substrate molecules for the catalytic sites showed that {*R*} and {*S*} should involve cavity structures that fit both templates and the substrate.

Table 1. Kinetic Parameters of the Inhibition Reactions with the Chiral Templates: Noncompetitive Inhibition and Enantioselective Competitive Inhibitions

Catalysts	K_m	V_{max}[a]	k_{cat}	k_{cat}/K_m	Inhibitors	K_i	$-\Delta G_0$[b]	$-\Delta\Delta G_0$[c]
	10^{-4}M[d]	$10^{-4}s^{-1}$	$10^{-1}s^{-1}$	M^{-1}		$10^{-6}M^{-1}$	kJ	kJ
					1 (*R*)[e]	7.53	29.71	0.66
{*R*}	6.98	1.11	9.65	13.8	**2** (*S*)	9.08	29.05	
					1 (*R*)	4.76	30.87	
{*S*}	10.10	2.13	15.96	15.8	**2** (*S*)	4.05	31.28	0.41
Control	19.5	1.71	15.40	7.90	**1,2** (*R*),(*S*)	81.05	—	—

a) Maximum of k_{obsd}. b) Molecular recognition capability. c) Chiral recognition capability. d) M=mol dm^{-3}. e) Configuration of the inhibitor molecule. f) Catalytic site molarity; 2.30×10^{-6} mol g^{-1}. g) 2.67×10^{-6} mol g^{-1}. h) 2.22×10^{-6} mol g^{-1}.

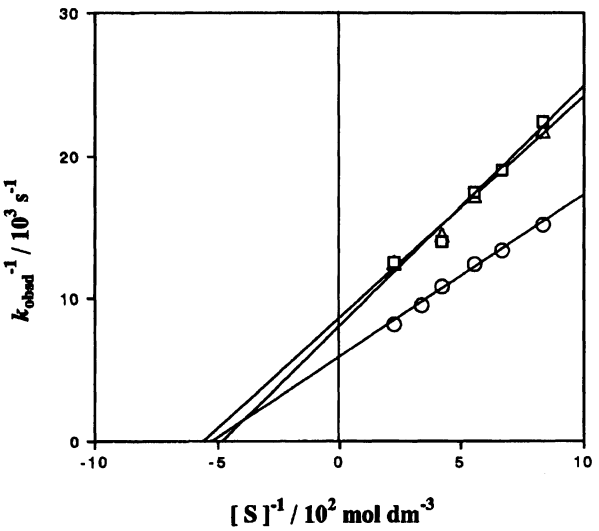

Fig. 2. Lineweaver–Burk plots for the catalyzed reactions with and without templates over the control gel catalyst. Noncompetitive inhibition. Open circle: Without the inhibitors. Open triangle: With (*R*)-template(inhibitor) **1**: [I]=4.00×10^{-5} mol dm^{-3}. Open square: With (*S*)-template(inhibitor) **2**; [I]= 4.00×10^{-5} mol dm^{-3}.

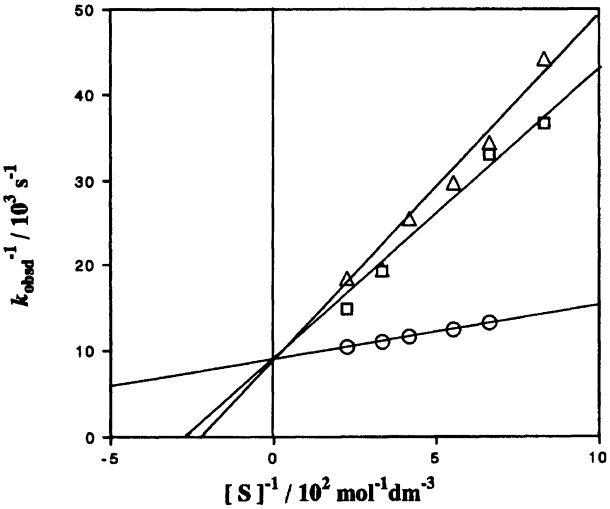

Fig. 3. Lineweaver–Burk plots for the catalyzed reactions with and without templates over the footprint cavities {*R*}. Competitive inhibition. Open circle: Without the inhibitors. Open triangle: With (*R*)-template(inhibitor) **1**; [I]=4.00×10^{-5} mol dm^{-3}. Open square: With (*S*)-template(inhibitor) **2**; [I]= 4.00×10^{-5} mol dm^{-3}.

Also, Figs. 3 and 4 clearly proved that enantioselective competitive inhibition occurred; (*R*)-inhibitor inhibited {*R*} more strongly than did (*S*)-inhibitor; (*R*)-inhibitor inhibited {*R*} more strongly than did (*S*)-inhibitor. This finding evidently supported the idea that chirally imprinted footprint cavities had chiral recognition capabilities due to their chiral cavity structures as expected. Table 1 summarizes the kinetic parameters of the catalyzed reactions. Since (*R*)- and (*S*)-templates are enantiomeric, {*R*} and {*S*} should reveal finely identical catalytic behavior except for symmetrically opposite enantioselectivities. The observed data in Table 1, however, are not so identical or symmetrical. This is because the imprintings are not always perfectly reproducible.[9] However, the rough estimation of the catalytic behavior would be sufficient to discuss the enantioselectivity in a semiquantitative way at this stage. A competitive inhibition provided a competitive inhibition constant, K_i. Then the magnitude of the molecular recognition capabilities could be measured by $-\Delta G_0 (=RT \ln K_i)$.[2] Also, the chiral recognition capability could be measured by $-\Delta\Delta G_0$, defined as the difference in $-\Delta G_0$ between the inhibitors of an enantiomer (Table 1). The observed chiral recognition capabilities of {*R*} and {*S*} (0.41—0.66 kJ) were moderate, not so large. They were less than that observed in the enantioselective catalysis of a hydantoinase mimic as previously reported,[9] where 1.18 kJ of the chiral recognition capability could be calculated from K_m values. These moderate chiral recognition capabilities could be explained from the structures of the cavities as follows. The chiral structures of the footprint cavities might be determined by the adsorption postures of the chiral template molecules on the Lewis acid sites during the imprinting process. A Stuart model examination sug-

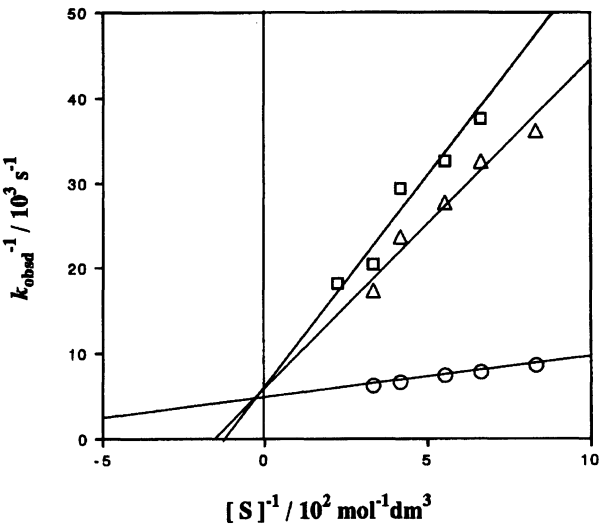

Fig. 4. Lineweaver–Burk plots for the catalyzed reactions with and without templates over the footprint cavities $\{S\}$. Competitive inhibition. Open circle: Without the inhibitors. Open triangle: With (R)-template(inhibitor) **1**; [I]=4.00×10^{-5} mol dm^{-3}. Open square: With (S)-template(inhibitor) **2**; [I]= 4.00×10^{-5} mol dm^{-3}.

gests two possible adsorption postures of the template molecules. So they provide two possible structures of footprint cavities (Type 1 and Type 2 in Scheme 2). The cavity of type 1 comprises a Lewis acid site (Al of aluminate) and three subsites (**a**, **b**, and **c**). Both subsites **a** and **c** are complementary to phenyl groups, and the subsite **b** is complementary to a methyl group. The cavity of type 2 also comprises a Lewis acid site and three subsites, **a**, **b′**, and **c**. Two of the subsites, **a** and **c**, are also complementary to phenyl groups, but the subsite **b′** is complementary to the hydrogen of the methine group in the template molecule. Scheme 2 schematically shows how the cavities $\{S\}$ of the two types rebind the chiral template as an inhibitor. When the (S)-template (inhibitor) molecule binds on the cavity $\{S\}$ of type 1, it takes the best fitting mode, which is the same posture as that in its imprinting process. When an (R)-template (inhibitor) molecule of the another configuration binds on the cavity $\{S\}$ of the type 1, the (R)-inhibitor molecule must take another binding posture as Scheme 2 shows. We assumed the subsites **a** and **c** preferentially accept the two phenyl groups of the (R)-inhibitor, and then the subsite **b** must accept the too small hydrogen of the methine group, instead of the best fitting methyl group. The excluded methyl group stands upright out of the cavity. The assumption of such preferential binding of the two phenyl groups is supported by our earlier study on the molecular recognition capability of footprint cavities; a subsite for a phenyl group showed much higher affinity to a phenyl group than that for a methyl group showed to a methyl group by about 14 kJ in n-butanol.[2] Such a binding posture that excludes the methyl group is sterically possible, but might be energetically less stable than the binding of (S)-inhibitor on $\{S\}$. This posture should show moderate enantioselective inhibition. When an (R)-inhibitor binds on $\{S\}$ of the type 2, no stable binding posture seems possible from a Stuart model examination, because subsite **b′** of the small capacity must reject the methyl group by steric hindrance. Such unstable binding should show exclusive enantioselective competitive inhibition in the mode of "all or nothing". The observed enantioselectivities of the inhibitors were not so exclusive but moderate. Therefore, the cavities $\{S\}$ and $\{R\}$ were likely of type 1. Furthermore, this presumption is reasonable from the viewpoint of the imprinting process using the template **1** or **2**. The hydrophobic phenyl and methyl groups of **1** or **2** might be transferred preferentially to the methine hydrogen from aqueous media onto the less polar silicate surface in the imprinting. Such an adsorption posture of the template forms the cavity structures of type 1, through the continuous rearrangement of the silicate matrix.[1,7] Also this assumed cavity formation for type 1 can be supported by findings in the similar imprintings with N-benzoyl-(N^{α}-benzyloxycarbonyl)-L-alaninamide (Z–L-Ala–NH–Bz),[11] bis(N-benzyloxy carbonyl-L-alanyl)amine ((Z–L-Ala)$_2$NH),[6] 5-phenyl-2,4-diketo-tetrahydro-oxazole,[12] and 5-phenyl-2,4-imidazolinedione (5-phenylhydantoin).[9] All of these imprintings provided similar subsites for the more hydrophobic methyl or phenyl groups instead for the methine hydrogen.

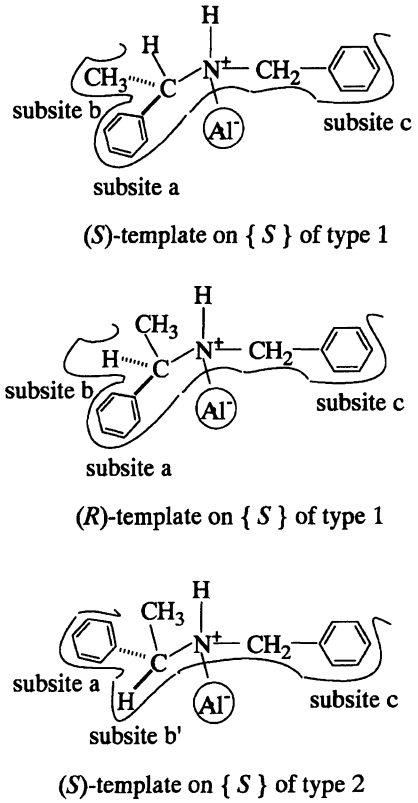

Scheme 2. Binding postures of templates and inhibitor.

Table 2. Kinetic Parameters of the Inhibition Reactions with the Chiral Templates: Enantioselective Uncompetitive Inhibitions

Catalysts	K_m	V_{max} [a]	k_{cat}	k_{cat}/K_m	Inhibitors	K_i	$-\Delta G_0$ [b]	$-\Delta\Delta G_0$ [c]
	10^{-4}M [d]	$10^{-4}s^{-1}$	$10^{-1}s^{-1}$	M^{-1}		$10^{-6}M^{-1}$	kJ	kJ
					3 (*R*) [e]	49.7	24.96	1.98
{*R*} [f]	10.40	1.25	11.21	10.80	**4** (*S*)	109.0	22.98	
					3 (*R*)	28.7	26.35	
{*S*} [g]	49.30	2.33	17.68	3.6	**4** (*S*)	17.3	27.62	1.27

a), b), c), d), and e) are the same as those in Table 1. f) Catalytic site molarity; 2.23×10^{-6} mol g^{-1}. g) 2.64×10^{-6} mol g^{-1}.

"Uncompetitive" Enantioselective Inhibition. The inhibition studies with chiral amines (*R*)- and (*S*)-α-methylbenzylamine **3** and **4** further clarified the cavity structures and the binding postures of the chiral inhibitors on the cavities. The chiral inhibitor **3** and **4** had partial structures in **1** and **2**. They should bind the cavities {*R*} and {*S*} to show the moderate enantioselectivities through binding with a Lewis acid site and subsites **a** and **b**, if the above assumed cavity structures were correct. Figures 5 and 6 show the Lineweaver–Burk plots for the catalyzed reactions of {*R*} and {*S*} under the presence of **3** and **4**. The plots show that the inhibitory effects of **3** and **4** were also clearly enantioselective throughout the entire range of the substrate concentration. The three plotting lines in Figs. 5 and 6, however, are obviously different from those in Figs. 3 and 4. They are parallel to each other. These patterns showed there occurred not simply competitive but "uncompetitive" inhibition. This uncompetitive inhibition appeared for the first time in our inhibition studies of the footprint catalysis (Table 2). According to enzymatic kinetics,[14] the uncompetitive inhibition occurrs when a catalytic site (E), a substrate molecule (S), and an inhibitor molecule (I) make a reversible ternary complex (E-S-I or E-I-S) in the catalyzed reaction process. Such a ternary complex should be formed in the chiral footprint cavity, and should explain the enantioselectivity thereon. A Stuart model examination supports the idea such a ternary complex is possible in the cavity as Scheme 3 shows, where the subsite **c** accepts a phenyl group of the substrate molecule and the subsites **a** and **b** accept the phenyl group and methyl group of the inhibitor, respectively. The Lewis acid site activates the carbonyl group to generate a carbonium cation. Then the cation can bind the amino group of the inhibitor to form a reversible tetrahedral intermediate. Such ternary complex formation is sterically possible in the cavity, if the cavity structures are such as those assumed above (Scheme 2, type 1). These binding postures explained the moderate enantioselective inhibitions with

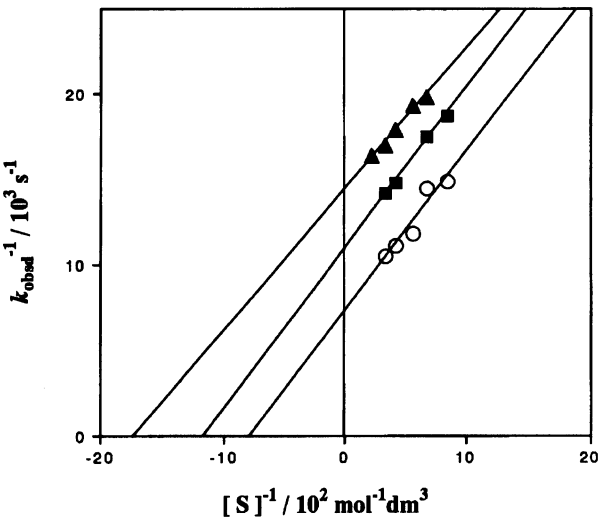

Fig. 5. Lineweaver–Burk plots for the catalyzed reactions with and without templates over the footprint cavities {*R*}. Uncompetitive inhibition. Open circle: Without the inhibitors. Closed triangle: With (*R*)-inhibitor **3**; [I]=4.00×10^{-5} mol dm^{-3}. Closed square: With (*S*)-inhibitor **4**; [I]=4.00×10^{-5} mol dm^{-3}.

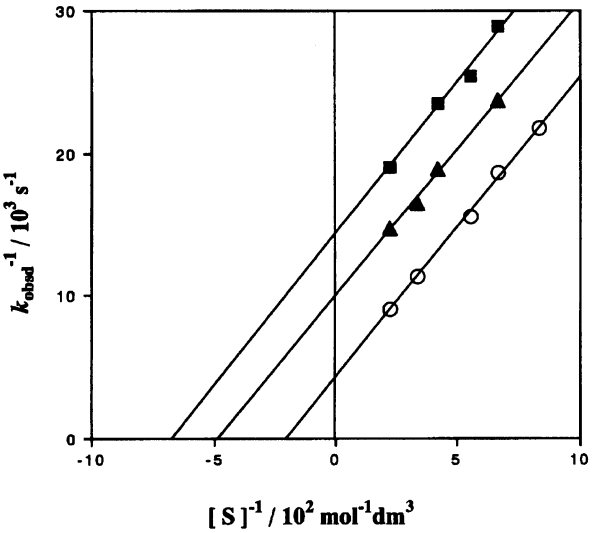

Fig. 6. Lineweaver–Burk plots for the catalyzed reactions with and without templates over the footprint cavities {*S*}. Uncompetitive inhibition. Open circle: Without the inhibitors. Closed triangle: With (*R*)-inhibitor **3**; [I]=4.00×10^{-5} mol dm^{-3}. Closed square: With (*S*)-inhibitor **4**; [I]=4.00×10^{-5} mol dm^{-3}.

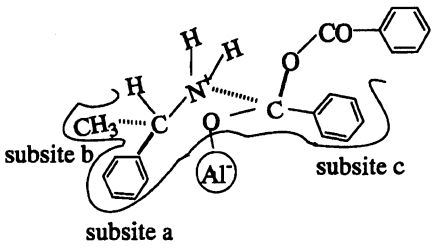

(*S*)-inhibitor and substrate on { *S* } of type 1

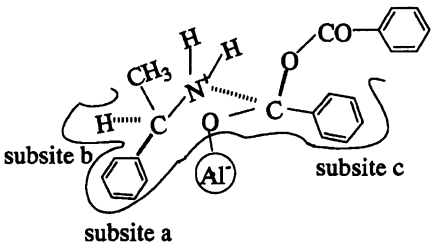

(*R*)-inhibitor and substrate on { *S* } of type 1

Scheme 3. Ternary complexes in uncompetitive inhibition.

the chiral amines **3** and **4**.

Concluding Remarks. Our imprinting method provided chirally imprinted cavities with use of chiral amines **1** and **2**. This was the first use of free base amines as templates; most of the templates used for the imprinting thus far were acylamines, diacylamines, and sulfonamide derivatives. The use of free base amines as templates would extend the scope of the template choice.

The chiral recognition capabilities for amines would afford an effective tool for analysis and separation of a stereoisomer from the enantiomeric amines. The footprint imprinting was a simple modification of a commercial silica gel, so that large scale preparation (more than 100 g) was easy. The imprinted gel preparation showed a high capacity for binding of $2—3\times10^{-5}$ mol g^{-1}, and a tight binding with K_i of 10^{-6} (mol dm^{-3}) order. Surface modification by trimethylsilylation with hexamethyldisilazane provided a hydrophobic and stable gel preparation that retained the molecular recognition capability of footprint cavities almost intact, diminishing nonspecific adsorption capability on the outer area of the cavities.[10] Such useful features of footprint cavities can be combined with the chiral selective capabilities. The most promising application of the footprint cavities might be specific adsorption of a stereoisomer rather than chromatographic separation.[13,15—19] The high capacities and strong affinities would effectively remove traces of a remaining stereoisomer from the amines once optically resolved for much higher optical purity. The finding of the ternary complex with a substrate and an inhibitor in the footprint cavity would lead the similar bisubstrate reaction system as those reported by T. R. Kelly et al. as "A Bisubstrate Reaction Template".[20] These varying application of the footprint cavities are now being undertaken.

References

1) Part I: K. Morihara, S. Kurihara, and J. Suzuki, *Bull. Chem. Soc. Jpn.*, **61**, 3991 (1988).
2) Part II: K. Morihara, E. Nishihara, M. Kojima, and S. Miyake, *Bull. Chem. Soc. Jpn.*, **61**, 3999 (1988).
3) Part III: K. Morihara, E. Tanaka, Y. Takeuchi, K. Miyazaki, N. Yamamoto, Y. Sagawa, E. Kawamoto, and T. Shimada, *Bull. Chem. Soc. Jpn.*, **62**, 499 (1989).
4) Part IV: T. Shimada, K. Nakanishi, and K. Morihara, *Bull. Chem. Soc. Jpn.*, **65**, 954 (1992).
5) Part V: T. Shimada, R. Kurazono, and K. Morihara, *Bull. Chem. Soc. Jpn.*, **66**, 836 (1993).
6) Part VI: K. Morihara, S. Kawasaki, M. Kofuji, and T. Shimada, *Bull. Chem. Soc. Jpn.*, **66**, 906 (1993).
7) Part VII: K. Morihara, S. Doi, M. Takiguchi, and T. Shimada, *Bull. Chem. Soc. Jpn.*, **66**, 2977 (1993).
8) Part VIII: K. Morihara, T. Iijima, H. Usui, and T. Shimada, *Bull. Chem. Soc. Jpn.*, **66**, 3047 (1993).
9) Part IX: T. Matsuishi, T. Shimada, and K. Morihara, *Bull. Chem. Soc. Jpn.*, **67**, 748 (1994).
10) Part X: T. Shimada, R. Hirose, and K. Morihara, *Bull. Chem. Soc. Jpn.*, **67**, 227 (1994).
11) K. Morihara, M. Kurokawa, Y. Kamata, and T. Shimada, *J. Chem. Soc., Chem. Commun.*, **1992**, 358.
12) T. Matsuishi, T. Shimada, and K. Morihara, *Chem. Lett.*, **1992**, 1921.
13) L. Fischer, R. Muller, B. Ekberk, and K. Mosbach, *J. Am. Chem. Soc.*, **113**, 9358 (1991).
14) E. Zeffren and P. Hall, "The Study of Enzyme Mechanisms," John Wiley & Sons, Inc., New York (1973), Chap. VI.
15) B. Sellergren, M. Lepistoe, and K. Mosbach, *J. Am. Chem. Soc.*, **110**, 5853 (1988).
16) B. Sellergren, B. Ekberk, and K. Mosbach, *J. Chromatogr.*, **347**, 1 (1985).
17) A. Sarhan, *Makromol. Chem.*, **190**, 2031 (1989).
18) L. I. Andersson and K. Mosbach, *J. Chromatogr.*, **516**, 313 (1990).
19) L. I. Andersson, A. Miyabayashi, D. J. O'Shannessy, and K. Mosbach, *J. Chromatogr.*, **516**, 323 (1990).
20) T. R. Kelly, C. Zhao, and G. J. Bridger, *J. Am. Chem. Soc.*, **111**, 3744 (1989).